References

[1]Hussain, A. K. M. F., and Zaman, K. B. M. Q., "Vortex Pairing in a Circular Jet Under Controlled Excitation. Pt. 2. Coherent Structure Dynamics," *Journal of Fluid Mechanics*, Vol. 101, No. 3, 1980, pp. 493–544.

[2]Yule, A. J., "Large Scale Structure in the Mixing Layer of a Round Jet," *Journal of Fluid Mechanics*, Vol. 89, No. 3, 1978, pp. 413–432.

[3]Bruun, H. H., "A Time Domain Analysis of the large Scale Flow Structure in a Circular Jet, Pt. 1. Moderate Reynolds Number," *Journal of Fluid Mechanics*, Vol. 83, No. 4, 1977, pp. 641–671.

[4]Zaman, K. B. M. Q., and Hussain, A. K. M. F., "Natural Large Scale Structures in the Axisymmetric Mixing Layer," *Journal of Fluid Mechanics*, Vol. 138, 1984, pp. 325–351.

[5]Oler, J. W., and Goldschmidt, V. W., "Coherent Structures in the Similarity Region of Two Dimensional Turbulent Jets," *Journal of Fluids Engineering*, Vol. 106, 1984, pp. 187–192.

[6]Aydore, S., Disimile, P. J., Tsuei, Y. G., and Behbahani, A. I., "Phase Averaged Vorticity Measurements in the Nearfield of a Self-Excited Impinging Jet," *Bulletin of the American Physical Society*, Vol. 35, No. 10, 1990, p. 2113.

[7]Aydore, S.,"Investigation of Large Coherent Structures in the Nearfield of an Impinging Axisymmetric Jet," Ph.D. Thesis, Div. of Graduate Studies and Research, Univ. of Cincinnati, OH, 1991.

Shrinkage Flow Effects on the Convective Stability of NH_4Cl-H_2O Directional Solidification

J. A. Hopkins,* T. D. McCay,† and M. H. McCay‡

University of Tennessee Space Institute, Tullahoma, Tennessee 37388-8897

Nomenclature

A = discretization matrix left-hand side
a = wavenumber, 1/cm
B = discretization matrix right-hand side
B_C = coefficient of solutal expansion, 1/wt%
B_T = coefficient of thermal expansion, 1/°C
C = solutal concentration, wt%
C_p = specific heat, J/g °C
C_t = dendrite tip solutal concentration, wt%
c = constant in permeability model
D = solutal diffusivity, cm^2/s
d = characteristic length for Forchheimer inertia term, cm
dl = length of solutal diffusion layer in all liquid region, cm
$d1$ = primary dendrite arm spacing, cm
F = Forchheimer inertia term, 1/cm
Gl = temperature gradient at solid-liquid interface, °C/cm
g = gravitational acceleration, cm/s^2
g_e = Earth's gravitational acceleration, 980 cm/s^2
k = partition coefficient
L_f = latent heat, J/g
m = liquidus slope, °C/wt%
P = pressure, $dynes/cm^2$
T = temperature, °C
t = time, s
u = fluid velocity in x direction, cm/s
V = solidification growth rate, cm/s
$\bar{V}$ = fluid velocity vector, cm/s
W, w = fluid velocity in z direction, cm/s
x = solution vector, W, T, C
y = horizontal coordinate normal to gravitational acceleration, cm
z = vertical coordinate parallel to gravitational acceleration, cm
zt = height of two-phase region, cm
zl = far-field distance, cm
α = thermal diffusivity, cm^2/s
γ = solidification shrinkage parameter, $(\rho_s - \rho_l)/\rho_s$
κ = permeability, cm^2
ν = kinematic viscosity, cm^2/s
ρ = density, g/cm^3
ρ_l = liquid density, g/cm^3
ρ_s = solid density, g/cm^3
σ = temporal growth parameter, 1/s
Φ = liquid fraction

Subscripts

0 = value at $z = 0$
∞ = far-field value
s = base state value

Superscripts

$'$ = perturbation value
$*$ = critical value

Received Dec. 14, 1992; presented as Paper 93-0261 at the AIAA 31st Aerospace Sciences Meeting, Reno, NV, Jan. 11–14, 1993; revision received Dec. 12, 1994; accepted for publication Jan. 9, 1995.

*Post Doctoral Research Associate, Center for Laser Applications.

†Vice President and Professor of Engineering Science and Mechanics, Center for Laser Applications.

‡Professor of Engineering Science and Mechanics, Center for Laser Applications.

Introduction

CONVECTIVE flows occurring during solidification have been studied extensively. For multicomponent systems, the flows are primarily a manifestation of density differences within the liquid arising from phase change solutal redistribution. The resulting fluid motion can have a dramatic consequence with respect to the results of the solidification process. Both constituent segregation and solid structure are influenced by convection, and significant effort has been expended in trying to model these effects.[1–11] Because convective flows create constituent segregation, i.e., channelling and freckling, within the final solid matrix, they are generally considered undesirable, and it is of interest to determine solidification conditions for which convective flows will not occur.

Background

The importance of gravity level for vertical directional solidification (VDS) has been examined using linear stability analyses by Nandapurkar et al.[9] Worster,[10,11] and Hopkins.[8] The importance of other parameters has also been examined. Neilson and Incropera[1] showed the effects of permeability on nonlinear convection during the solidification of Pb-Sn. Worster[10,11] used a novel linear model to show the effects of permeability and Prandtl number, among other parameters, on the transition. He found two regimes for the breakdown, one associated with the fluid layer and the other associated with the mushy zone. Hopkins[8] examined the influence of the two-phase region on breakdown, performing both linear stability calculations and experiments. Each of these studies illustrated the importance of one or more parameters on the transition to convection for VDS. The study reported here emphasizes the importance of a factor which has received little attention, shrinkage flow.

The physical situation associated with the convective stability of the melt for a solidifying system is as follows. A solutal diffusion layer develops within and in front of the growing two-phase mushy zone, and, if the solute is less dense than the bulk fluid, the potential for buoyant flow exists. Figure 1 shows the temperature, solute, and density profiles for this situation. For stability calculations concerning many materials (including the NH_4Cl-H_2O discussed here), it is of interest to determine to what degree the shrinkage flow influences the transition to convective flow.

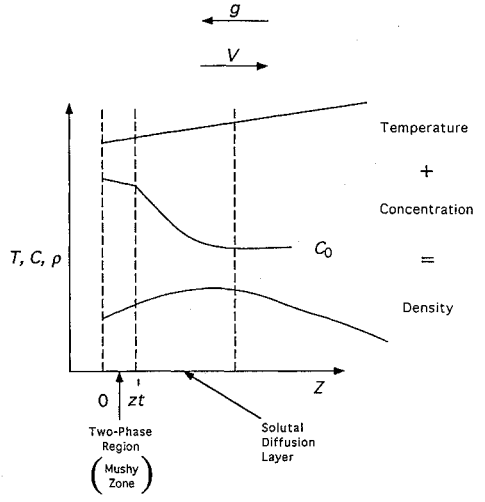

Fig. 1 Temperature, solute, and density profiles for VDS with light solute rejection.

To this end, the VDS of NH_4Cl-H_2O under Bridgman-type conditions has previously been examined[8,12–14] both experimentally and numerically to show that the onset of convection for this process manifests itself as the transition from a state with a well-defined, undisturbed solutal diffusion layer to well-defined, stationary convection cells. Extensive analysis[8,14] of the diffusion layer, both before and at the onset of convection, showed that two-phase momentum effects play the major role in determining the point of breakdown.

This paper expands on these results, showing the individual effect that shrinkage flow has on the onset of convection during the VDS of NH_4Cl-H_2O.

Approach

A linear stability analysis was used to predict the onset of convection for the VDS of an NH_4Cl-72 wt% H_2O solution. Normal mode expansion was used to represent the perturbation solution, and finite difference approximations for a grid clustered around the solid-liquid interface were employed to approximate the resulting eighth-order ordinary differential equation (ODE) system.

The domain used for the calculations is semi-infinite in the z direction and infinite in the x direction. Because of the influence of the two-phase region on convective flows, Darcy extended conservation equations were used; This included a typical linear (velocity dependence) Darcy friction term and a nonlinear Forchheimer term. Because the experimentally measured fraction of liquid ranges from 0.9 to 1 in this problem, the viscous dissipation term was retained. A Boussinesq approximation was used, hence, properties for each phase were constant throughout the domain, and density for each phase was constant except for the body force term in the z-direction momentum equation. The resulting equations referenced to a coordinate system moving with velocity V are

$$\frac{\partial u}{\partial x}+\frac{\partial w}{\partial z}=\gamma\frac{\partial \Phi}{\partial t}-\gamma V\frac{\partial \Phi}{\partial z} \tag{1}$$

$$\frac{\partial u}{\partial t}-V\frac{\partial u}{\partial z}=-\frac{\Phi}{\rho_0}\frac{\partial P}{\partial x}+\nu\nabla^2 u-\frac{\nu\Phi}{\kappa}u-F\Phi|\bar{V}|u \tag{2}$$

$$\frac{\partial w}{\partial t}-V\frac{\partial w}{\partial z}=-\frac{\Phi}{\rho_0}\frac{\partial P}{\partial z}+\nu\nabla^2 w-\frac{\nu\Phi}{\kappa}w-\Phi\frac{\rho}{\rho_0}g-F\Phi|\bar{V}|w \tag{3}$$

$$\frac{\partial T}{\partial t}-V\frac{\partial T}{\partial z}+u\frac{\partial T}{\partial x}+w\frac{\partial T}{\partial z}=\alpha\nabla^2 T-\frac{L_f}{C_p}\frac{\partial \Phi}{\partial t}+V\frac{L_f}{C_p}\frac{\partial \Phi}{\partial z} \tag{4}$$

$$\Phi\frac{\partial C}{\partial t}-V\Phi\frac{\partial C}{\partial z}+u\frac{\partial C}{\partial x}+w\frac{\partial C}{\partial z}=D\left[\frac{\partial}{\partial x}\left(\Phi\frac{\partial C}{\partial x}\right)+\frac{\partial}{\partial z}\left(\Phi\frac{\partial C}{\partial z}\right)\right]-\frac{(1-k)}{(1-\gamma)}\frac{\partial \Phi}{\partial t}C+V\frac{(1-k)}{(1-\gamma)}\frac{\partial \Phi}{\partial z}C \tag{5}$$

with boundary conditions for $z = 0$:

$$T=T_0,\qquad C=C_0,\qquad u=w=0 \tag{6a}$$

and for $z = zt + zl$:

$$T=T_\infty,\qquad C=C_\infty,\qquad u=w=0 \tag{6b}$$

The domain is defined such that zl is an integer multiple of the characteristic solutal diffusion layer length D/V with initial solute conditions at the far boundary. This assured that the zero perturbation far-field boundary condition would be satisfied. F is defined as

$$F=1.75(1-\Phi)/\Phi^3 d \tag{7}$$

where d is a characteristic dimension of the porous region. The permeability relation used in this study

$$\kappa=cd_1^2\Phi^3/(1-\Phi^2) \tag{8}$$

was developed experimentally by Poirier[15] for the dendritic Pb-Sn system and is valid for flow parallel to the primary dendrite arms. In this equation $d1$ is the primary dendrite arm spacing and c is an empirical constant. Equation (8) was used in conjunction with data appropriate for NH_4Cl-H_2O (Ref. 8).

The governing equations defining the base state for the mushy-zone region are

$$\frac{dw_s}{dz}=-\gamma V\frac{d\Phi_s}{dz} \tag{9}$$

$$\frac{\partial P_s}{\partial x}=0 \tag{10}$$

$$-V\frac{dw_s}{dz}+\frac{w_s}{\Phi_s}\frac{dw_s}{dz}=-\frac{\Phi_s}{\rho_0}\frac{dP_s}{dz}+\nu\frac{d^2 w_s}{dz^2}-\frac{\nu\Phi_s}{\kappa_s}w_s-\Phi_s\frac{\rho}{\rho_s}g-F_s\Phi_s(w_s)^2 \tag{11}$$

$$\frac{d^2T_s}{dz^2}+\frac{(w_s-V)}{\alpha}\frac{dT_s}{dz}+\frac{VL_f}{c_p\alpha}\frac{d\Phi_s}{dz}=0 \tag{12}$$

$$\frac{d^2C_s}{dz^2}+\frac{(w_s-V)}{D}\frac{dC_s}{dz}+\frac{1}{\Phi_s}\frac{d\Phi_s}{dz}\frac{dC_s}{dz}+\frac{(1-k)}{(1-\gamma)}\frac{V}{\Phi_s D}\frac{d\Phi_s}{dz}C_s=0 \tag{13}$$

$$T=T_m+mC \tag{14}$$

with the boundary conditions

$$\Phi_s(zt)=1,\qquad C_s(zt)=C_t,\qquad \left(\frac{dC_s}{dz}\right)_{zt}=\frac{1}{m}Gl,\qquad w_s(0)=0 \tag{15}$$

It is noted that the $w_s(0) = 0$ velocity boundary condition is a pertinent simplification of $w_s(0) = -\gamma V[1 - \Phi_s(0)]$ due to the high fraction of liquid values for this study. It is also convenient for removing the additional difficulty in solving the nonzero boundary condition.

The base state equations and boundary conditions for the fluid-only layer simplify to

$$\frac{d^2T_s}{dz^2} + \frac{w_s - V}{\alpha}\frac{dT_s}{dz} = 0, \qquad T_s(zt) = T_t$$
$$\left(\frac{dT_s}{dz}\right)_{zt} = Gl \tag{16}$$

$$\frac{d^2C_s}{dz^2} + \frac{w_s - V}{D}\frac{dC_s}{dz} = 0$$
$$C_s(zt) = C_t, \qquad C_s(zt + zl) = C_\infty \tag{17}$$

$$\frac{dw_s}{dz} = 0 \tag{18}$$

The mushy-zone equations reduced to a boundary value problem in w_s, Φ_s, C_s, and T_s, which was solved iteratively using Runge–Kutta integration. The equations in the fully liquid region were readily solved to complete the base state definition.

The variables u, w, P, T, C, and ρ were then written in terms of base state and perturbation quantities. These were substituted into the original equations and base state and nonlinear perturbation terms were removed. Pressure was removed from the equations by taking the curl of the momentum equation and using the continuity equation. The resulting perturbation variables, w', T', and C' were expressed in terms of a normal mode expansion

$$w'(x, z, t) = W(z)e^{(\sigma t + iax)}$$
$$T'(x, z, t) = T(z)e^{(\sigma t + iax)} \tag{19}$$
$$C'(x, z, t) = C(z)e^{(\sigma t + iax)}$$

where a is the spatial wave number of the perturbation.

The perturbation density was written in terms of perturbation temperature and concentration as

$$\rho' = B_T T' + B_C C' \tag{20}$$

to yield the following linear, eighth-order ordinary differential equation system:

$$\frac{d^4W}{dz^4} + \left(\frac{V}{\nu} - \frac{1}{\Phi_s}\frac{d\Phi_s}{dz}\right)\frac{d^3W}{dz^3}$$
$$+ \left(\frac{F_s\Phi_s}{\nu}w_s - \frac{V}{\nu\Phi_s}\frac{d\Phi_s}{dz} - 2a^2 - \frac{\Phi_s}{\kappa_s}\right)\frac{d^2W}{dz^2}$$
$$+ \left(\frac{1}{\nu\Phi_s}\frac{dF_s w_s \Phi_s}{dz} + \frac{F_s w_s}{\nu}\frac{d\Phi_s}{dz} + \frac{a^2}{\Phi_s}\frac{d\Phi_s}{dz}\right.$$
$$\left. + \frac{1}{\kappa_s}\frac{d\Phi_s}{dz} - \frac{Va^2}{\nu} - \frac{d\Phi_s/\kappa}{dz}\right)\frac{dW}{dz}$$
$$+ \left(a^4 + \frac{F_s\Phi_s w_s a^2}{\nu} + \frac{\Phi_s a^2}{\kappa_s}\right)W - \frac{g\Phi_s a^2}{\nu}(B_c C + B_T T)$$
$$= \sigma\left(\frac{-1}{\nu}\frac{d^2W}{dz^2} + \frac{1}{\nu\Phi_s}\frac{dW}{dz} - \frac{a^2}{\nu}W\right) \tag{21}$$

$$\frac{d^2T}{dz^2} + \left(\frac{w_s - V}{\alpha}\right)\frac{dT}{dz} - a^2T - \frac{1}{\alpha}\frac{dT_s}{dz}W = \sigma T \tag{22}$$

$$\frac{d^2C}{dz^2} + \left[\frac{(w_s/\Phi_s) - V}{D} + \frac{1}{\Phi_s}\frac{d\Phi_s}{dz}\right]\frac{dC}{dz}$$
$$+ \left[\frac{(1-k)}{(1-\gamma)}\frac{V}{D\Phi_s}\frac{d\Phi_s}{dz} - a^2\right]C - \frac{1}{D\Phi_s}\frac{dC_s}{dz}W = \sigma C \tag{23}$$

This system was approximated using second-order accurate (first order at the boundaries) finite differences for a Gl point grid with points clustered at the solid-liquid interface. This was necessary to resolve the large spatial variations in the coefficients arising from the two-phase momentum terms. The resulting generalized eigensystem, $Ax = \sigma Bx$, was solved for the neutral stability case (the onset of convection) by setting $\sigma = 0$ and examining the system $Ax = 0$. The determinant of A will be zero for conditions satisfying the case of neutral stability. The determinant of A was, thus, calculated for various values of wave number and either temperature gradient or dendrite tip concentration, and curves in (a, C_t) space were constructed that represent the neutral stability state. The corresponding minimum C_t values for these curves are the critical stability values for the specified problem.

Results

A set of calculations was performed for which the mushy-zone height, solutal diffusion layer length, and temperature gradient were known. This approximates a quasisteady solidification process that has been previously investigated experimentally.[8]

The experiments were shown to undergo transition to convection before eutectic boundary conditions could be established at $z = 0$. Therefore, for a given growth velocity V, applied temperature gradient Gl, two-phase region height zt, and liquid region height, zl, the linear stability model was used to examine the stability of the system by iterating on the solutal concentration at the dendrite tips. Because growth velocity was known, the base state tip concentration was not given by the physical boundary condition arising from the steady-state growth equation but was dictated by the linear stability model (LSM) as an iteration variable. Because the value of C_t used

Table 1 Property values and two-phase constants

ν	=	9.82×10^{-3} cm^2/s	D	=	2.3×10^{-5} cm^2/s
c_p	=	2.83 kJ/kg °C	α	=	1.5×10^{-3} cm^2/s
L_f	=	277 kJ/kg	c	=	4.7×10^{-4}
m	=	−4.69 °C/wt%	d	=	5 μm
k	=	0.003	$d1$	=	50 μm

Table 2 Growth conditions

zt	=	0.05 cm
dl	=	0.05 cm
zl	=	0.50 cm
V	=	5×10^{-5} cm/s
Gl	=	10 °C/cm

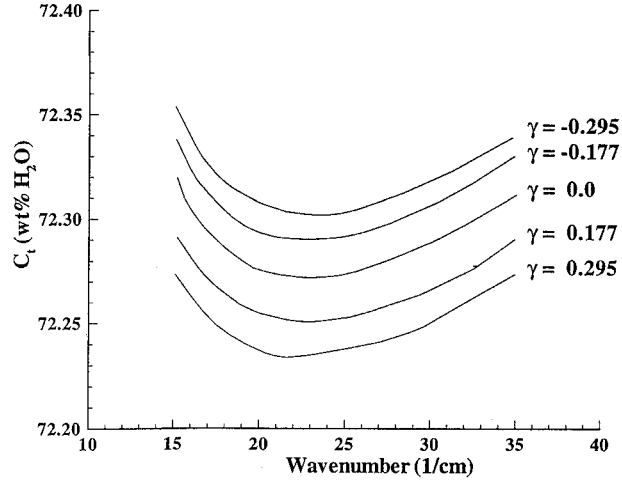

Fig. 2 Neutral stability curves as a function of shrinkage parameter for quasisteady VDS.

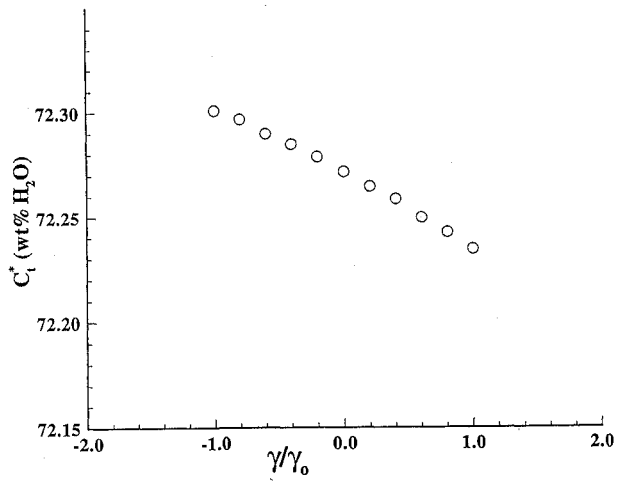

Fig. 3 Critical dendrite tip concentration as a function of shrinkage parameter for quasisteady VDS.

in the iterations is not necessarily that given by the steady-state boundary condition, the term quasisteady is used to describe this approach.

The model was used with the property values and growth conditions of Tables 1 and 2, respectively.

Figure 2 presents selected neutral stability curves for various levels of shrinkage/expansion flow, and Fig. 3 illustrates the dependence of critical dendrite tip concentration on such flow. A shrinkage flow in the direction opposite that of the solidification direction tends to make the system more susceptible to convective breakdown, and an expansion flow tends to stabilize the system. There is a 14% difference between the stability criteria predicted for the case with shrinkage flow ($\gamma = 0.295$) as opposed to the case with no shrinkage flow ($\gamma = 0$).

Conclusions

The effects of shrinkage flow are significant in determining the onset of convection during VDS of NH_4Cl-H_2O. Shrinkage flow was found to be destabilizing if in the direction opposite solidification, and stabilizing if in the direction of solidification. A difference of 14% was found between stability criteria for cases with and without shrinkage flow illustrating the importance of including the difference in phase densities in studies of convection during phase change processes.

Acknowledgments

Funding for this work was provided through the NASA Office of Space Sciences and Applications under NAS8-37293. Rudy Ruff is the technical monitor.

References

[1]Neilson, D. G., and Incropera, F. P., "Unidirectional Solidification of a Binary Alloy and the Effects of Induced Fluid Motion," *International Journal of Heat and Mass Transfer*, Vol. 34, No. 7, 1991, pp. 1717–1732.

[2]Beckermann, C., and Viskanta, R., "Double-Diffusive Convection During Dendritic Solidification of a Binary Mixture," *Physico-Chemical Hydrodynamics*, Vol. 10, No. 2, 1988, pp. 195–213.

[3]Voller, V. R., Brent, A. D., and Prakash, C., "The Modelling of Heat, Mass, and Solute Transport in Solidification Systems," *International Journal of Heat and Mass Transfer*, Vol. 32, No. 9, 1989, pp. 1719–1731.

[4]Poirier, D. R., Nandapurkar, P. J., Heinrich, J. C., and Felicelli, S., "Convection During Directional Solidification of Dendritic Alloys," *Materials Science Forum*, Vol. 50, Sept. 1988, pp. 65–78.

[5]Prescott, P. J., and Incropera, F. P., "Numerical Simulation of a Solidifying Pb-Sn Alloy: The Effects of Cooling Rate on Thermosolutal Convection and Macrosegregation," *Metallurgical Transactions*, Vol. 22B, Aug. 1991, pp. 529–540.

[6]Oldenburg, C. M., and Spera, F. J., "Numerical Modelling of Solidification and Convection in a Viscous Pure Binary Eutectic System," *International Journal of Heat and Mass Transfer*, Vol. 34, No. 8, 1991, pp. 2107–2121.

[7]Felicelli, S. D., Heinrich, J. C., and Poirier, D. A., "Simulation of Freckles During Vertical Solidification of Binary Alloys," *Metallurgical Transactions*, Vol. 22B, Dec. 1991, pp. 847–859.

[8]Hopkins, J. A., "Onset of Convection During Vertical Directional Dendritic Solidification and the Stabilizing Effect of the Two-Phase Region," Ph.D. Dissertation, Dept. of Mechanical Engineering, Univ. of Tennessee, Knoxville, TN, May 1992.

[9]Nandapurkar, P., Poirier, D. R., Heinrich, J. C., and Felicelli, S., "Thermosolutal Convection During Dendritic Solidification of Alloys: Part I. Linear Stability Analysis," *Metallurgical Transactions*, Vol. 20B, Oct. 1989, pp. 711–721.

[10]Worster, M. G., "Instabilities of the Liquid and Mushy Regions During Solidification of Alloys," *Journal of Fluid Mechanics*, Vol. 237, April 1992, pp. 649–669.

[11]Worster, M. G., "Natural Convection in a Mushy Layer," *Journal of Fluid Mechanics*, Vol. 224, March 1991, pp. 335–359.

[12]McCay, T. D., McCay, M. H., and Gray, P. A., "Experimental Observations of Convective Breakdown During Directional Solidification," *Physical Review Letters*, Vol. 62, No. 17, 1989, pp. 2060–2063.

[13]McCay, T. D., McCay, M. H., Lowry, S. A., and Smith, L. M., "Convective Instabilities During Directional Solidification," *Journal of Thermophysics and Heat Transfer*, Vol. 3, No. 3, 1989, pp. 345–350.

[14]Hopkins, J. A., McCay, T. D., and McCay, M. H., "Interferometric Measurements of a Dendritic Growth Front Solutal Diffusion Layer," AIAA Paper 91-1334, June 1991.

[15]Poirier, D. R., "Permeability for Flow of Interdendritic Liquid in Columnar-Dendritic Alloys," *Metallurgical Transactions*, Vol. 18B, March 1987, pp. 245–255.

Evaluating the Temporal Accuracy of Inlet Normal Shock Propagation Simulations

Gerald C. Paynter*
Boeing Commercial Airplane Group, Seattle, Washington 98124-2207
and
David W. Mayer†
Boeing Defense and Space Group, Seattle, Washington 98124-2207

Introduction

ATMOSPHERIC disturbances encountered by a high-speed civil transport (HSCT) may induce an inlet unstart (expulsion of the normal shock) depending on the magnitude of the disturbance and the unstart tolerance of the inlet/engine combination. The NPARC[1] flow simulation software is being used to evaluate the unstart properties of a variety of inlet concepts, to support wind-tunnel tests aimed at evaluating inlet stability, and to support design of the inlet control system. Development of appropriate boundary conditions for unsteady Euler/Navier–Stokes inlet flow simulations has been under way for some time.[2,3] Now that appropriate boundary conditions are available for these simulations, the numerical time accuracy of the code for these tasks has become an important issue. Although NPARC can in theory be used to produce time-accurate

Received Oct. 3, 1994; revision received Feb. 24, 1995; accepted for publication March 6, 1995.

*Boeing Associate Technical Fellow, Propulsion Research Staff, Engineering Division. Associate Fellow AIAA.

†Senior Specialist Engineer, Propulsion Technology Staff, Military Airplane Division. Senior Member AIAA.